CHARGE EXCHANGE FLUXES OF RIPPLE TRAPPED SLOWING-DOWN IONS DURING L-to-H TRANSITION AND ELMs

Winfried Herrmann et al.

IPP 1/288 June 1995

MAX-PLANCK-INSTITUT FÜR PLASMAPHYSIK

85748 GARCHING BEI MÜNCHEN

MAX-PLANCK-INSTITUT FÜR PLASMAPHYSIK

GARCHING BEI MÜNCHEN

CHARGE EXCHANGE FLUXES OF RIPPLE TRAPPED SLOWING-DOWN IONS DURING L-to-H TRANSITION AND ELMs

Winfried Herrmann et al.

IPP 1/288 June 1995

Die nachstehende Arbeit wurde im Rahmen des Vertrages zwischen dem Max-Planck-Institut für Plasmaphysik und der Europäischen Atomgemeinschaft über die Zusammenarbeit auf dem Gebiete der Plasmaphysik durchgeführt.

Charge Exchange Fluxes of Ripple Trapped Slowing-down Ions during L-to-H Transition and ELMs

Winfried Herrmann, H.-U. Fahrbach, M. Kaufmann, K. Lackner, F. Ryter, H. Zohm, M. Albrecht, M. Alexander, K. Asmussen, K. Behler, K. Behringer, M. Bessenrodt-Weberpals, H.-S. Bosch, K. Büchl, A. Carlson, D. Coster, H.J. de Blank, R. Drube, R. Dux, W. Engelhardt, O. Gehre, J. Gernhardt, O. Gruber, G. Haas, A. Herrmann, S. Hirsch, P. Ignacz, B. Jüttner, W. Junker, A. Kallenbach, T. Kass, W. Köppendörfer, B. Kurzan, P.T. Lang, R.S. Lang, M. Laux, M. Maraschek, K.-F. Mast, H.-M. Mayer, D. Meisel, R. Merkel, V. Mertens, H. Murmann, B. Napiontek, D. Naujoks, G. Neu, R. Neu, J. Neuhauser, J.-M. Noterdaeme, G. Pautasso, S. de Pena Hempel, W. Poschenrieder, G. Raupp, H. Richter, H. Röhr, H. Salzmann, W. Sandmann, H.-B. Schilling, M. Schittenhelm, R. Schneider, W. Schneider, K. Schönmann, G. Schramm, U. Seidel, M. Sokoll, E. Speth, A. Stäbler, K.-H. Steuer, J. Stober, B. Streibl, W. Suttrop, W. Treutterer, M. Troppmann, M. Ulrich, H. Vernickel, O. Vollmer, H. Wedler, M. Weinlich, U. Wenzel, F. Wesner, R. Wunderlich, D. Zasche, H.-P. Zehrfeld.

Max-Planck-Institut für Plasmaphysik, D-85748 Garching, FRG
Euratom Association

Abstract

Neutral fluxes from charge exchange with ripple-trapped particles show a remarkably different behaviour during L and H mode; their measurement provides a new diagnostic for the mode discrimination of the plasma. A possible reason for the changes of the fluxes is the action of a radial electric field. This seems to grow steadily after the L-to-H transition with a strong increase (jump in the ms range) at the transition to the quiescent H-mode. During ELMs the fluxes reduce to L-mode level. Measurements with 100 μ time resolution show no action in the fluxes prior to the change in the D_α-signal at the start of type I ELM.

Since the discovery of the H-mode in ASDEX[1] many ideas have been published in an attempt to explain why the plasma switches from the low-confinement L-mode to the high-confinement H-mode and which plasma properties are of importance in this bifurcation process. For an intensive discussion and a list of references see, for example,[2,12]. The interest in this question derives its importance from the fact that the achievement of the H-mode is fundamental to the present-day concepts of a fusion reactor. A physical understanding of the processes involved would put extrapolations on a safer basis.

One of the main ingredients in many theories about the L-to-H transition is the development and behaviour of a radial electric field at the edge of the plasma, [3,4,5] whose shear could suppress fluctuations [6,7,11] and explain the improvement of confinement in H-mode by the development of a heat conduction and particle diffusion barrier. Electric fields perpendicular to a magnetic flux surface have been measured, especially on DIII- D, from the poloidal rotation of impurity ions [8,9,10] as well as of the basic plasma constituent [9].

These measurements show a distinct difference in the electric field profiles in the L- and H-modes. The electric field is negative in H-mode, with a level of shear sufficient to suppress fluctuations. The time resolution of these spectroscopic measurements seems to be limited to not much less than a millisecond. To shed more light on and eventually decide on the causality in the L-to-H transition, better time resolutions are essential. Surprisingly, it turns out, and this will be the subject of this paper, that fluxes from neutrals that result from charge exchange (cx) with slowing-down ions from neutral injection and that have scattered into the ripple-trapped domain can contain information about electric fields in the plasma. The time resolution can be shorter than $100\mu s$, the limitation resulting from the analyzer counting capability and from the intrinsic timescale of the particle trajectories in the plasma.

The cx analyzer of ASDEX Upgrade was set to detect neutrals, which belong to the class of mirror-trapped particles before charge exchange. Because of the fast grad B drift of energetic particles, these orbits should be almost unpopulated in the plasma. Only after the development of perpendicular electric fields could they remain in the plasma and, after charge exchange, be detected by the analyzer. Times to scatter particles from banana orbits to mirror trapped orbits are in the range of 10μs.

A description of the measuring system will be given in a more detailed publication. The analyzer is one of the devices built for JET by the Frascati Laboratory [13]. Figure 1 shows the D_α and cx-signals for ASDEX Upgrade shot 4998 for a time window around the L-to-H transition, a quiescent H-phase and first type-I ELMs. The uppermost trace is the D_α signal, which usually serves for discrimination of the modes. At time $t_1 = 1.6$ s a deuterium heating beam with about 2.6 MW is injected into a deuterium plasma with a current of I = 1000 kA and a central field of B = -2.1 T (drift towards the X-point). The acceleration voltage of the beams is 62 KV and the species mix $D_1/D_2/D_3$ about 60/17/23. The slowing-down time of the full energy ions lies in the range of 10 ms.

The average plasma density increases from $\bar{n} = 4.5 \cdot 10^{19} m^{-3}$ in L-mode to $\bar{n} = 6.7 \cdot 10^{19} m^{-3}$ in H-mode. The plasma transits from L- to H-mode at $t_2 = 1.648$ s, develops some noisy pattern - probably non-resolved type-III ELMs or dither - and enters a quiescent H*-mode at about $t_3 = 1.665$ s. The first type-I ELM appears at $t_4 = 1.754$ s.

The other traces in the figure show 8 channels of the CX analyzer for the neutral energies given at the left side of the figure. After injection of the beam the signal level increases but reaches a stationary low value during L-mode. After the transition the signal level again starts to increase, the earlier the lower the energy of the neutrals. In a broad energy range the fluxes show a "jump" at the transition

to the quiet H*-phase. The flux of the 20.1 keV neutrals increases only shortly before the first ELMs. During the ELMs the fluxes of the particles with the higher (non-thermal) energies reduce to about the signal level in L-mode.

The flux of neutral particles F(E) is determined by the following relation:

$$F(E) = k(E) \int n_i(E,r) \cdot n_0(r) \cdot \eta(E,r) dr,$$

where k(E) takes into account geometrical factors, the charge exchange rate and sensitivity factors of the analyzer, n_i (E,r) is the density of slowing-down particles of energy E at radius r in a phase space seen by the analyzer, n_o (r) is the local neutral density, and $\eta(E,r)$ the penetration probability of the neutrals through the plasma to the analyzer. There are two distinct possibilities for changes in F: reaction of n_i, n_0, η to changes in the plasma density n_e and plasma temperature T, and the change of n_i due to changing orbit effects under the influence of an electric field. We assume here, as generally accepted, that the slowing-down process is collision-dominated. A correct estimate of the first possibility should take into account the spatial deposition and slowing-down of the injected neutral beam, as a function of n_e and T together with the dependance of n_0 and η on these parameters. Full information on these quantities is difficult to get. Rough estimates show that density and temperature variations in the L-to-H transition and during ELMs could explain a factor of about 2 in the fluxes. The fact that the flux of the slowing-down particles increases after the transition contradicts the expectation based on the increased ion and electron densities and consequently reduced neutral density. The changes in fluxes can be an order of magnitude larger than estimated above. Figure 2 presents the ratio of the fluxes for times during and between ELMs as a function of the energy of the neutrals. Not only is the ratio in a broad energy range larger than can be explained by the estimate of the plasma influence, but also it is not nearly constant as a function of the energies, as would be expected

for changes in plasma background. The same argument holds for the increase of the fluxes after the L-to-H transition. This is quite different for the different energies, which is rather difficult to explain by changes in the plasma background. These drastic changes in the fluxes can, however, be explained if an electric field, perpendicular to the flux surfaces is assumed in the neighbourhood of the separatrix. Figure 3 shows a plot of a model electric field that was constructed according to measurements on DIII-D [14] for an ASDEX-Upgrade geometry as a function of the major radius a few cm above the geometrical midplane. Here the assumption has been made that the electric potential is constant on flux surfaces. The potential is also plotted in the figure. By using this electric field and the full information of the magnetic field from equilibrium calculations, including the magnetic ripple [15], the history of such ions, as could enter the analyzer after a charge exchange collision, was calculated for different electric field strengths.

Figure 4 shows the result of these trajectory calculations. For all shown trajectories deuterons with an energy of 20 keV start at $\rho_{pol} = 0.875$ (about 6 cm inside the separatrix) and 0.14 m above midplane. In reality, this is the endpoint of the particle because of charge exchange. For discrimination of the different trajectories they are plotted with a shift in radial direction. Trace a is without an electric field, traces b and c are for maximum electric fields of 7.9 and 15.9 kV/m. These trajectories should be unpopulated in the plasma because they represent loss trajectories. Trace d is for 23.8 kV/m. This electric field is high enough to confine the particles inside the separatrix. This is true also of higher fields, as assumed for trace e. Further calculations have confirmed the expectation that the electric field necessary to confine particles scales with their energy.

The whole effect of the measurement is based on the fact that the analyzer sees specifically ripple-trapped particles, which at least for higher energies are lost in a grad B-drift time scale as long as no electric field prevents the loss.

Calculations of the heating beam deposition and of the trajectories of the injected neutral beam deuterons show that a large fraction of them is concentrated at the outer part of the plasma, where the field ripple is effective.

These considerations lead us to conclude that the main structures of the CX signal, as shown in fig. 1, are indeed caused by a radial electric field. This grows steadily after the L/H-transition with a jump in the ms range at the transition to the quiet H*-phase. There is no indication in this shot for a jump at the L/H-transition, in agreement with measurements in ASDEX [17].

Because of the electric field the energy spectra of neutrals originating from ripple-trapped ions develop specific shapes for the different modes of the plasma. In fig. 5 the different spectral curves represent different modes and different development stages of the modes for the shot, whose fluxes are given in fig. 1. Curve a is taken at the end of the L-mode, curve b at the beginning of the H-mode, and c at the end of it, curve d at the beginning of the quiet phase of the H*-mode and curve e just before the first ELM. These curves suggest that the electric field grows in time and confines ripple-trapped particles with increasing energy. The low-energy points represent particles from the background plasma. The increase of their fluxes in time is related to the increase in plasma density and possibly also neutral density, connected with neutral injection. Curve e together with results of the calculation shown in fig. 4 suggests that the electric field has reached a value in the range of 20 kV/m.

The form of the curves in fig. 5 is a representative signature of the plasma mode. Especially curve a and e can be taken as signature for the L- and H-modes. It is also interesting to study the behaviour of the electric field during type-I ELMs. In fig. 6 the energy spectra are plotted at different time slices during an ELM. Curve a gives the flux integrated over the first ms after the start of the ELM. The curves

b to d show the fluxes during the following milliseconds. The signatures of the spectra at the start of the ELM and after the end of it are obviously

the signatures of the L- and H-modes. The conclusion that the type-I ELMs revert to L-mode may be overinterpreting the data. It seems undoubtful, however, that the radial electric field after the beginning of an ELM falls to low levels observed also in L-mode. Figure 7 compares the fluxes at 11.2 keV with a time resolution of 100μs during an ELM with the D_α signal (time resolution 25μs). The flux and hence the electric field decay in a time of less than or about 100μs. Obviously there is no action of the electric field prior to the steep increase in D_α.

The signature of the slowing-down particles undoubtedly determines the mode of the plasma, when the D_α diagnostic does not give clear mode identification like in the CDH (completely detached H)-phases [16]. This also indicates that the radial electric fields also persist in these phases. That also the ELMs persist in CDH-phases can be seen from the correlation of the fluctuations in the fluxes for different energies. Although the high frequency of the ELMs in these cases prevented their resolution in time, common aliasing effects in the fluxes leads to correlation in the fluxes if ELMs are present. The correlation analysis gives mode identification consistent with that from the spectral signature and other diagnostics.

1) F. Wagner, G. Becker, K. Behringer, et al., Phys. Rev. Lett. **49**, 1408, (1982).

2) K.H. Burrel, E.J. Doyle, P. Gohil, et al., Phys. Plasmas, **1**, 1536 (1994).

3) K.C. Shaing and E.C. Crume, Jr., Phys. Rev. Lett. **63**, 2369, (1989).

4) R.J. Taylor, M.L. Brown, B.D. Fried, et al., Phys. Rev. Lett. **63**, 2365, (1989).

5) S.-I. Itoh and K. Itoh, Phys. Rev. Lett. **60**, 2276, (1988).

6) H. Biglari, P.H. Diamond, and P.W. Terry, Phys. Fluids **B2**, 1, (1990).

7) K.C. Shaing, E.C. Crume, Jr., and W.A. Houlberg, Phys. Fluids **B2**, 1492, (1990).

8) R.J. Groebner, K.H. Burrell, and R.P. Seraydarian, Phys. Rev. Lett. **64**, 3015, (1990).

9) J. Kim, K.H. Burrell, P. Gohil, et al., Phys. Rev. Lett. **72**, 2199 (1994).

10) K. Ida, S. Hidekuma, Y. Miura, et al. Phys. Rev. Lett. **65**, 1364 (1990).

11) H. Matsumoto, K.H. Burrel et al., Plasma Phys. Control. Fusion, **34** (1992), p. 615

12) J. Hugill, Plasma Phys. Control. Fusion **36** (1994), B173

13) R. Bartiromo, G. Bracco et al., Rev. Sci. Instrum. **58**, 788 (1987).

14) P. Gohil, K.H. Burrell et al., 21st European Conf. on Controlled Fusion and Plasma Physics, Montpellier, France, Vol. 18b, Part II, p. 858, (1994).

15) The magnetic field due to the ripple in ASDEX Upgrade was put into a parametrized form by C. Hoffmann, IPP.

16) M. Kaufmann et al., 15th Intern. Conf. on Plasma Physics and Controlled Nuclear Fusion Research, Seville, Spain (1994), IAEA-CN-60/A-4-I-1.

17) A.R. Field, G. Fussmann, J.V. Hofmann et al., Nucl. Fus. **32**, 1191 (1992).

Figure Captions

Fig.1: D_α and neutral fluxes at different energies around the time of transition from L- to H-mode, (shot 4998).

Fig.2: Ratio of the pulse rates during and between ELMs as a function of the energy.

Fig.3: Solid and dotted lines: radial and vertical electric fields. Dashed line: negative value of the potential, 10 x increased.

Fig.4: Poloidal cross-section of ASDEX Upgrade and trajectories of ripple-trapped particles for different electric field strengths. a: 0 kV/m; b: -7.9 kV/m; c: -15.9 kV/m; d: -23.8 kV/m; e: -31.7 kV/m. Deuteron energy: 20kV. Blocking of the loss-cone occurs for fields around 20 kV/m. Trajectories and separatrix are displaced in the direction, marked "radius". The separatrix for each trajectory is at the same radial position.

Fig.5: Energy spectra for different phases of the L-to-H transition for the shot of Fig. 1. a: L-mode 1.635 s to 1.644 s: b: early H-mode 1.645 s to 1.655 s; c: late H-mode 1.680 s to 1.688 s; d: early H^*-mode, 1.690 s to 1.70 s; e: late H^*-mode, 1.757 s to 1.76 s.

Fig.6: Energy spectra during an ELM (see fig.7). a: 2.04 s to 2.0405 s; b: 2.041 s to 2.0415 s; c: 2.042 s to 2.0425 s. d: 2.043 s to 2.044 s. The spectrum during a type-I ELM has L-mode character.

Fig.7: Solid line: D_α signal (inverted, 25 μs time resolution); dotted line: CX signal for 11.2 keV particles (100 μs time resolution): no evidence of electric field action before the jump in D_αm, (shot 4998).

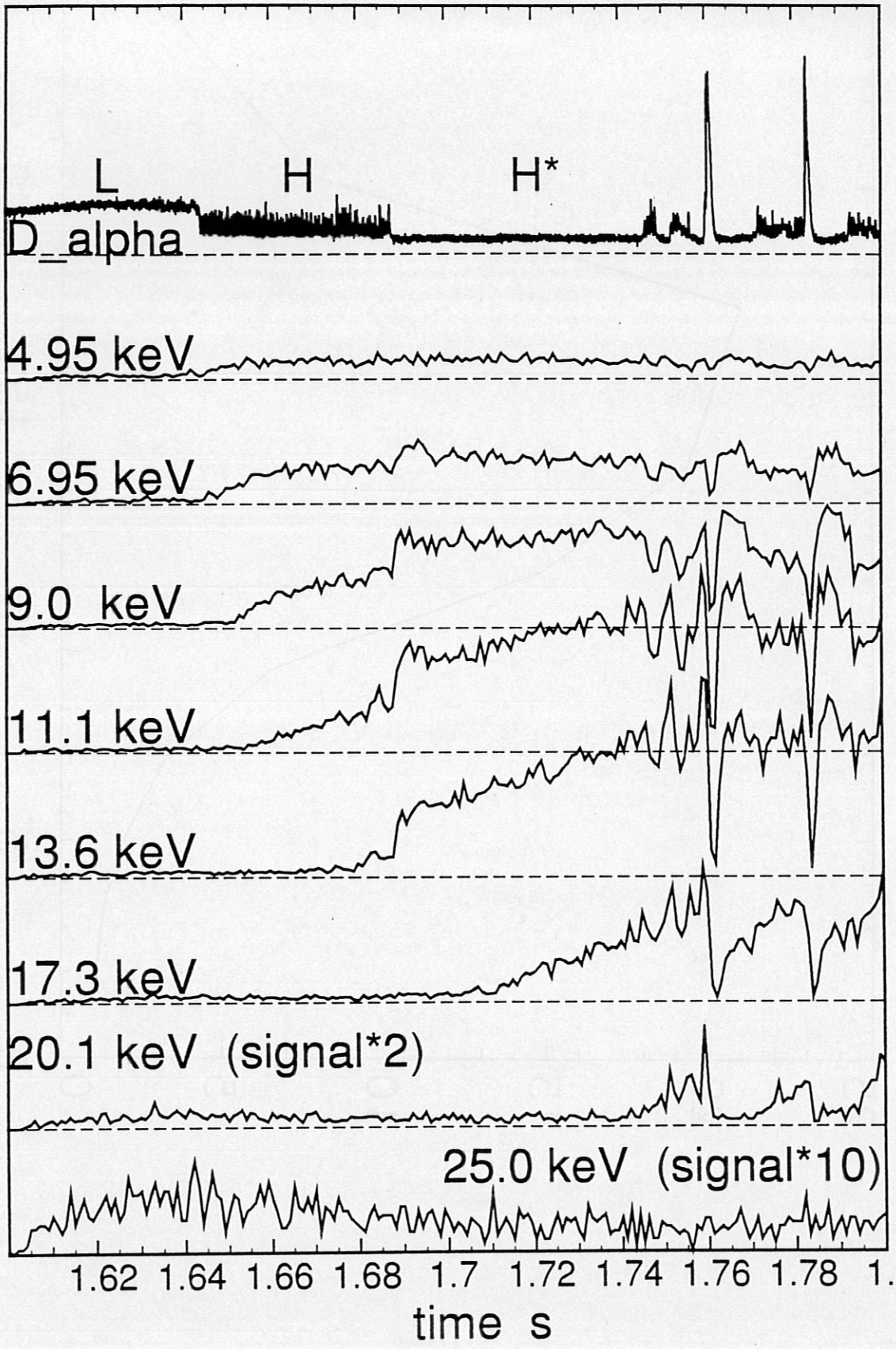
L
H
H*
D_alpha
4.95 keV
6.95 keV
9.0 keV
11.1 keV
13.6 keV
17.3 keV
20.1 keV (signal*2)
25.0 keV (signal*10)
1.62 1.64 1.66 1.68 1.7 1.72 1.74 1.76 1.78 1.8
time s

Fig. 1

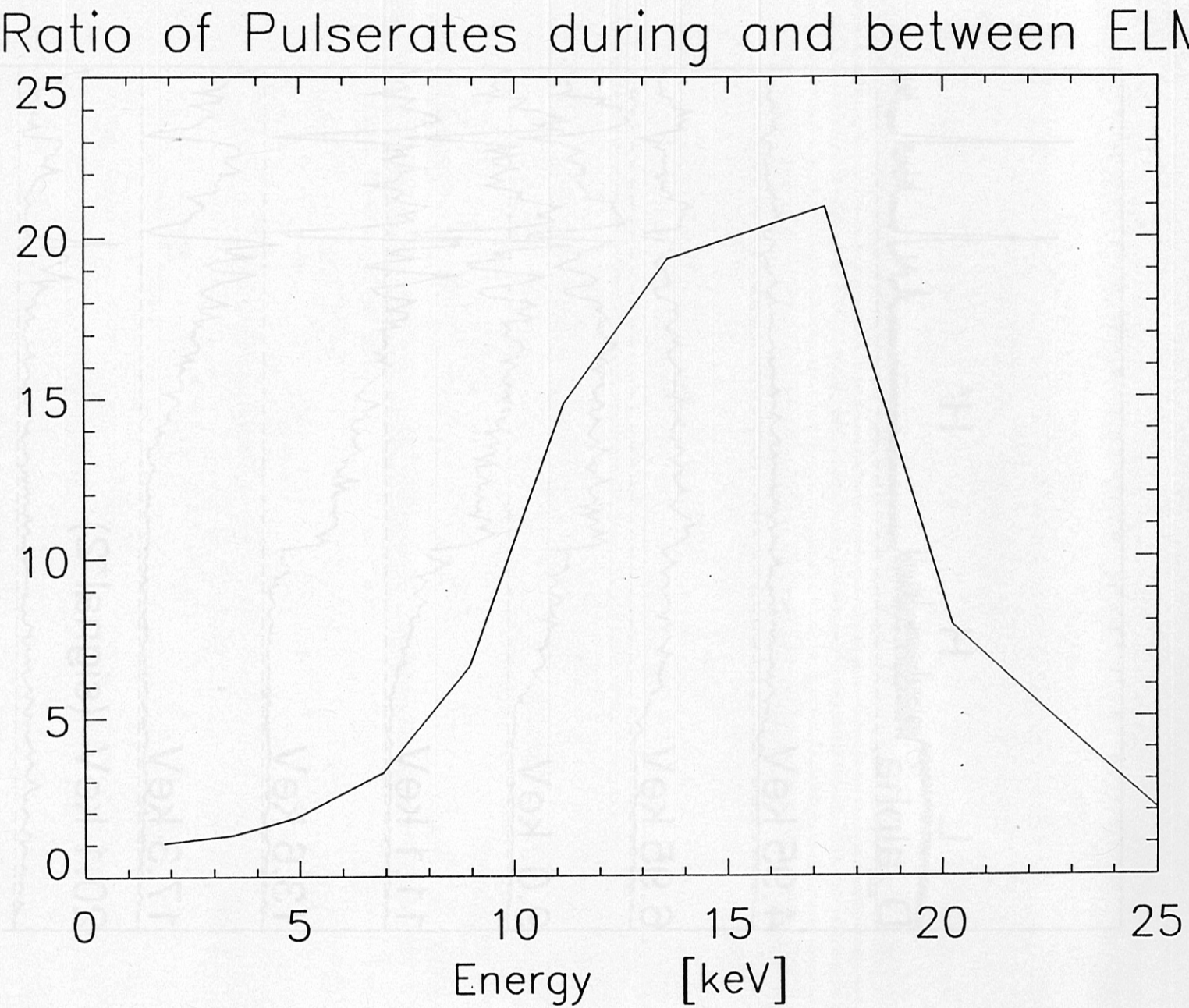
Ratio of Pulserates during and between ELMs
25
20
15
10
5
0
0
5
10
15
20
25
Energy [keV]

Fig. 2

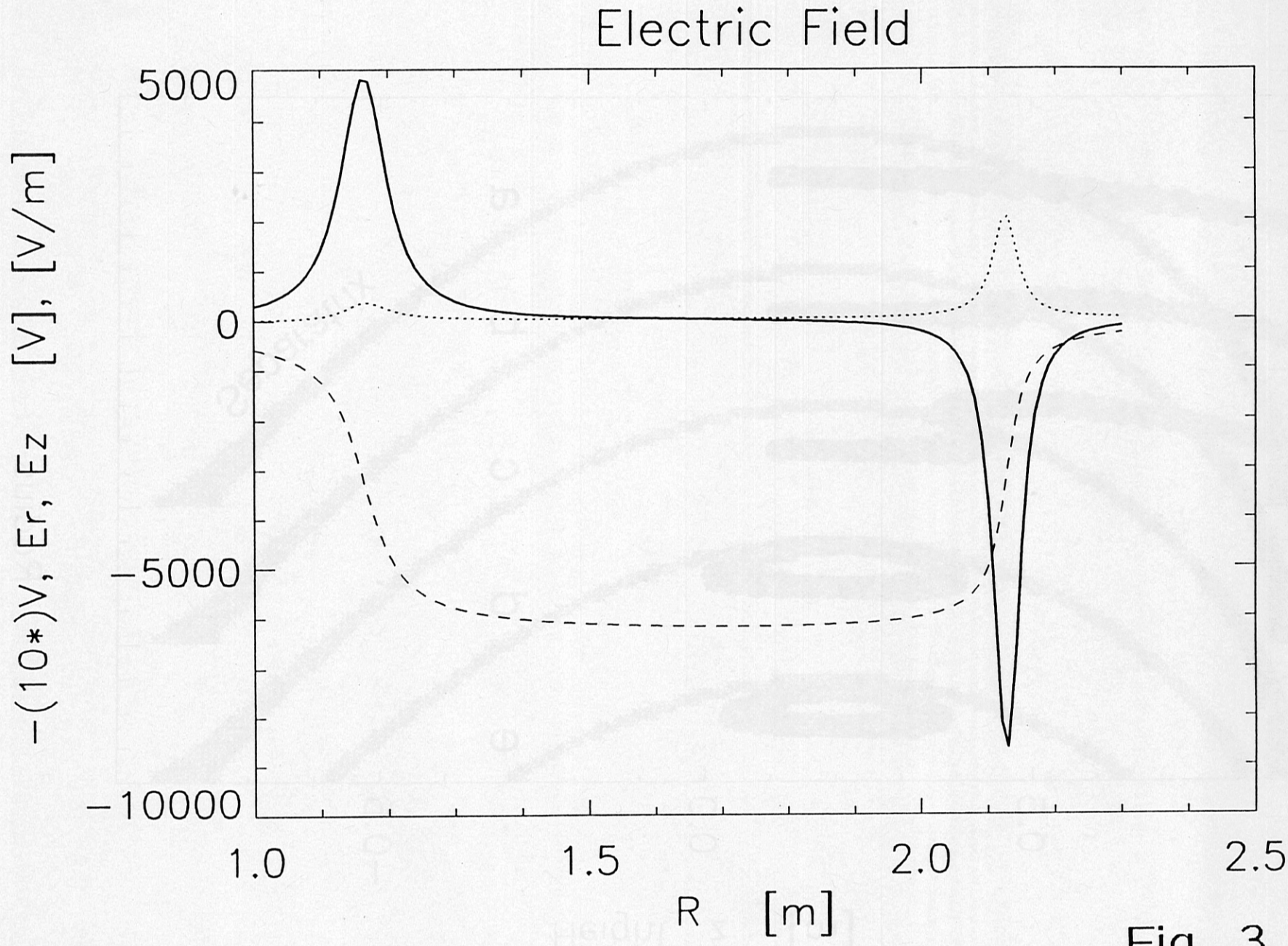

Fig. 3

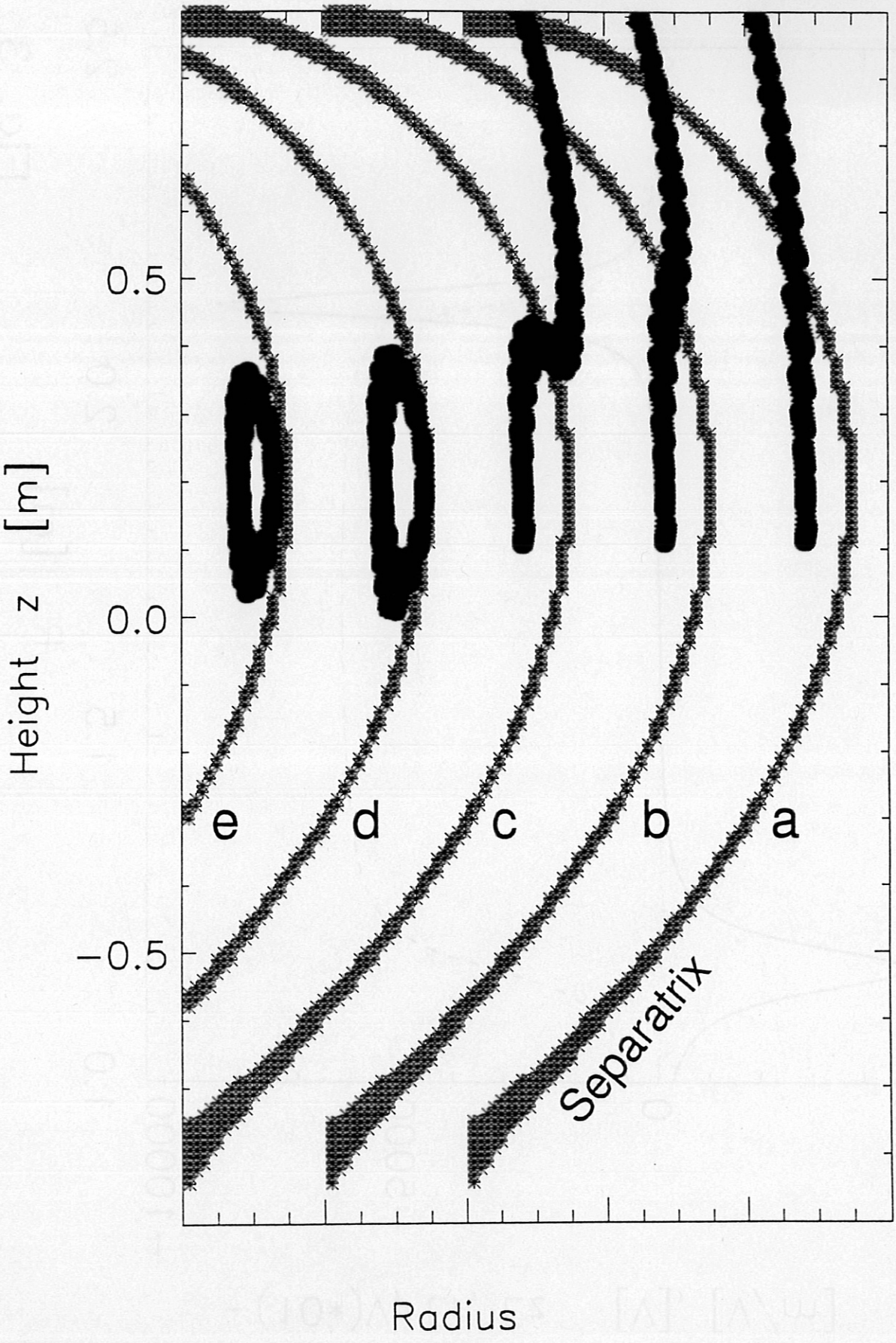

Fig. 4

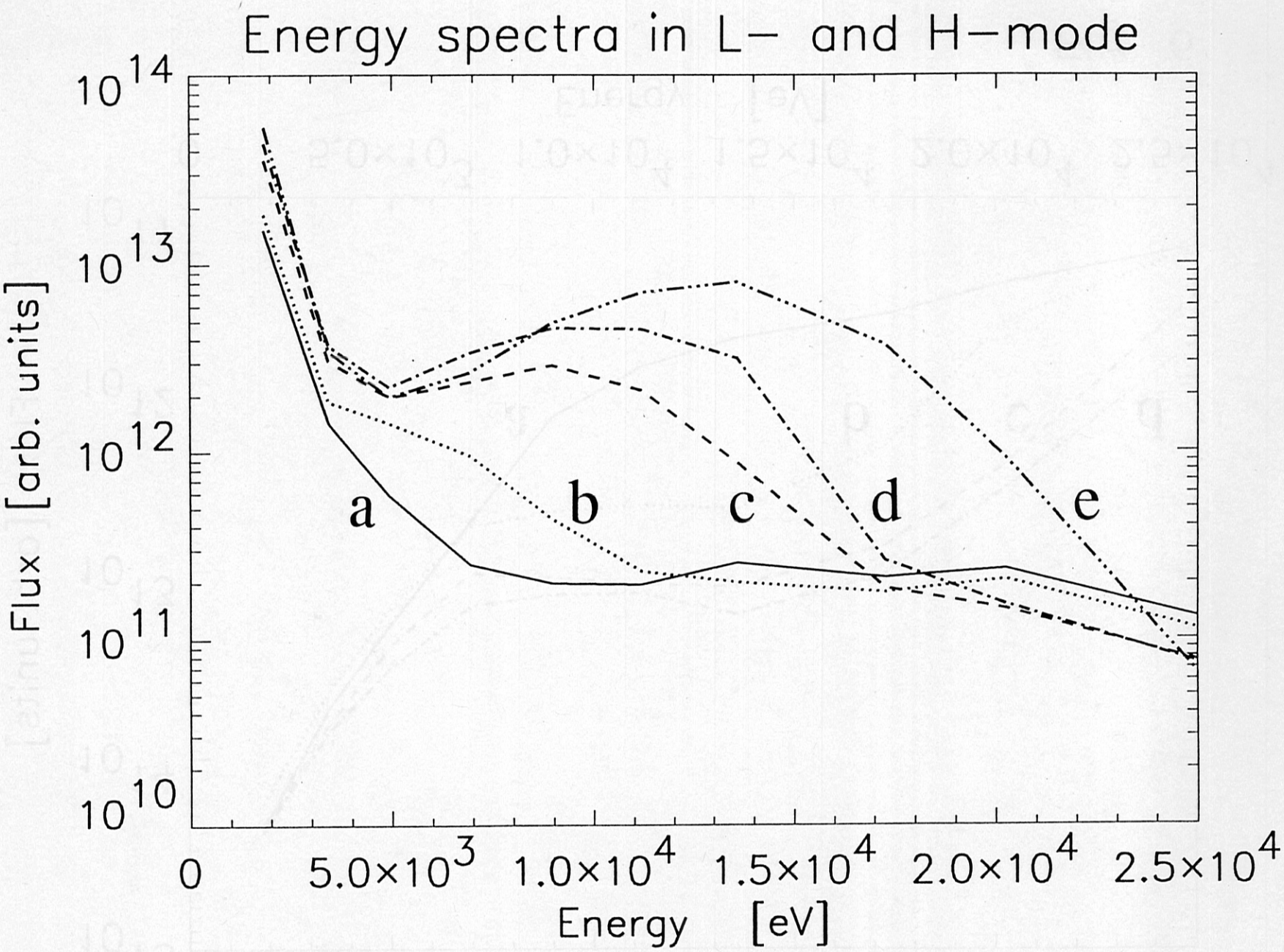
Energy spectra in L– and H–mode
Flux [arb. units]
10^14
10^13
10^12
10^11
10^10
a
b
c
d
e
0
5.0×10^3
1.0×10^4
1.5×10^4
2.0×10^4
2.5×10^4
Energy [eV]

Fig. 5

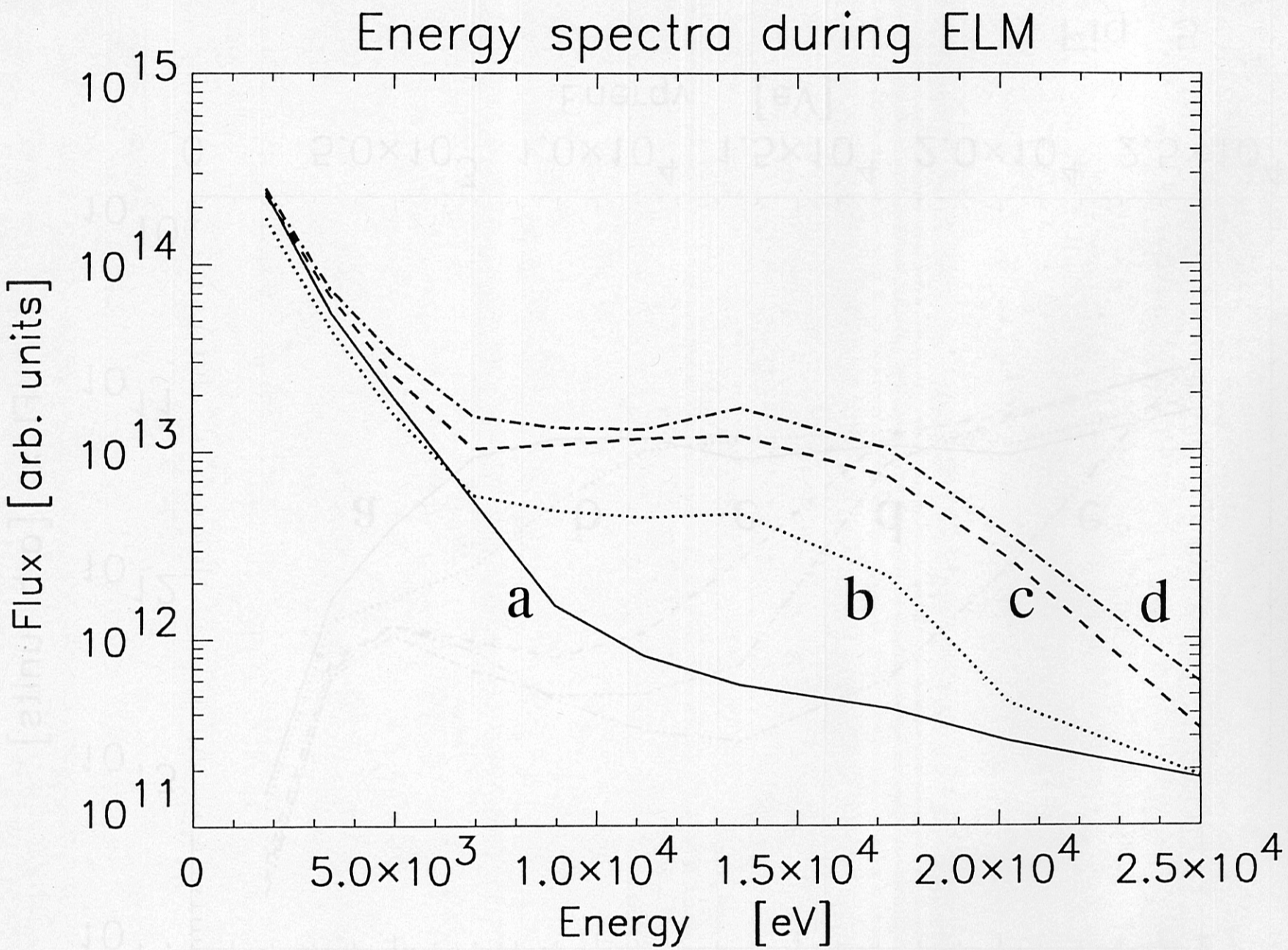
Energy spectra during ELM
Flux [arb. units]
10^{15}
10^{14}
10^{13}
10^{12}
10^{11}
a
b
c
d
0
5.0×10^{3}
1.0×10^{4}
1.5×10^{4}
2.0×10^{4}
2.5×10^{4}
Energy [eV]

Fig. 6

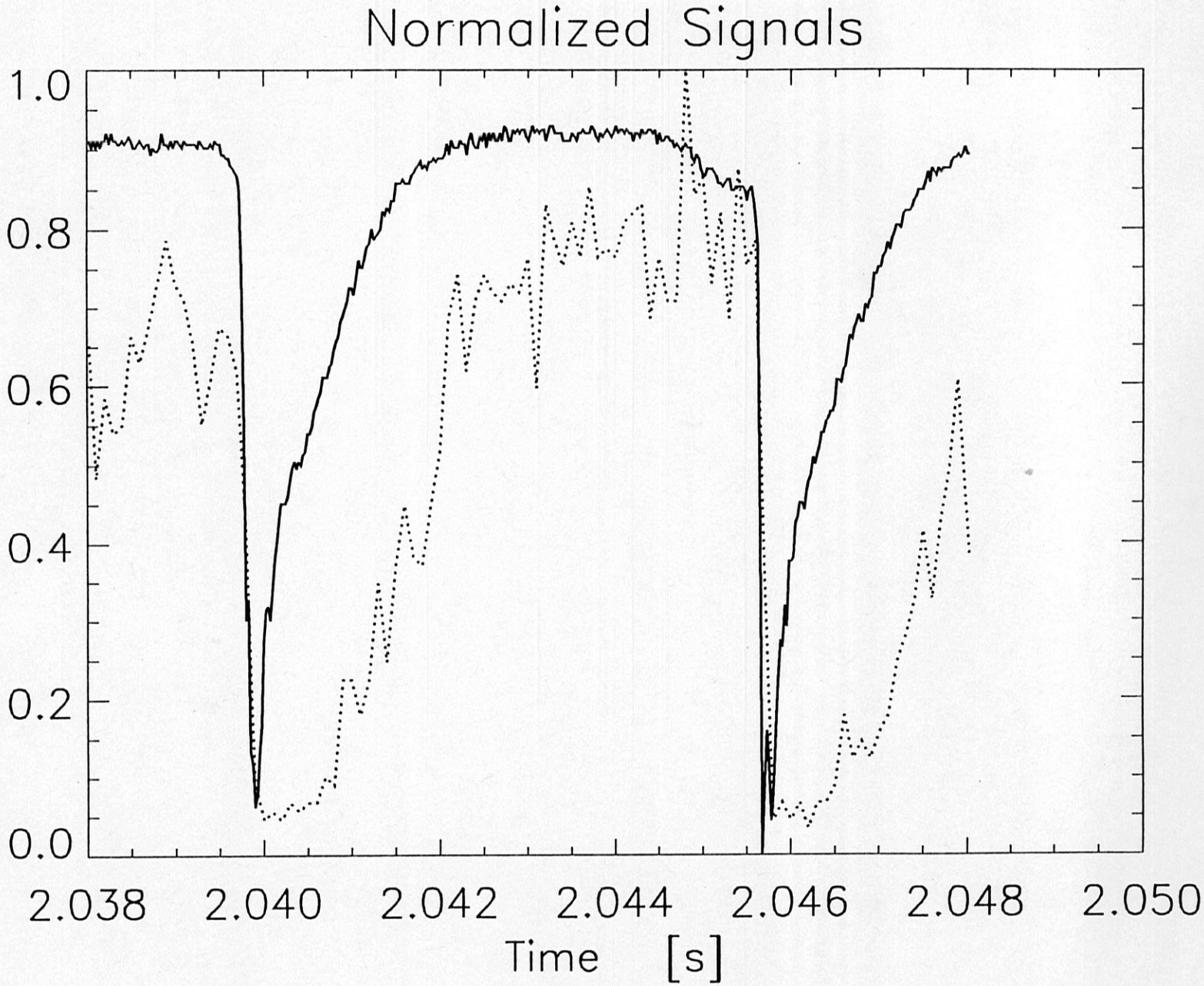
Normalized Signals
1.0
0.8
0.6
0.4
0.2
0.0
2.038
2.040
2.042
2.044
2.046
2.048
2.050
Time [s]

Fig. 7